Nucleus accumbens neuron subtype translatome signatures in socially stressed females

Gautam Kumar[1], Daniela Franco[1], Mahashweta Basu[2], Jimmy Olusakin[1], Rianne Campbell[1], Seth A. Ament[2,3,4], Megan E. Fox[4] Mary Kay Lobo[1,4*]

1. University of Maryland School of Medicine, Department of Neurobiology
2. Institute for Genome Sciences, University of Maryland School of Medicine
3. Maryland Psychiatric Research Center, Department of Psychiatry, University of Maryland School of Medicine
4. UM-MIND Institute for Neuroscience Discovery, University of Maryland School of Medicine
5. Penn State College of Medicine, Department of Anesthesiology & Perioperative Medicine

*Correspondence should be addressed to: mklobo@som.umaryland.edu

Word Count: 3997

Abstract

Background: The nucleus accumbens (NAc) is a reward circuitry hub associated with major depressive disorder (MDD) and chronic stress in rodents. While transcriptional adaptations in NAc medium spiny neuron (MSN) subtypes, those enriched in dopamine receptor 1(D1) or dopamine receptor 2 (D2) and adenosine 2a receptor (A2A) are well characterized in socially stressed male rodents, there is less knowledge of MSN subtype adaptations in socially stressed females.

Methods: Chronic witness defeat stress (CWDS) was performed in female D1-Cre-RiboTag and A2A-Cre-RiboTag mice. After stress, mice were separated into high- and low-social interactors with a three Chamber Social Interaction test. Following isolation of ribosome-associated mRNA, MSN subtype-specific gene expression profiles were determined with RNA sequencing followed by differential gene expression analysis (DEG) and weighted gene co-expression network analysis (WGCNA). Consensus WGCNA with male mouse social defeat stress and clinically relevant human transcriptomic datasets was performed to examine the translational sex-specific molecular signatures.

Results: 9 DEGs in D1-MSNs and 630 in A2A-MSNs were identified in female stress groups (FDR < 0.05). D1-MSN DEGs were mostly upregulated in CWDS low vs high interactors and were enriched for functions related to energy homeostasis and cell adhesion. A2A-MSN DEGs upregulated in low interactors involved structural molecules while downregulated genes involved neurotransmission. WGCNA identified 9 significant D1- and 5 significant A2A-MSN modules related to cell structure, protein synthesis, synapse and mitochondria. The most impacted modules from each subtype (based on DEG count) were enriched for PI3K-Akt-mTOR signaling pathway and regulated by the Nf1 transcription factor. Consensus module analysis identified a module significantly associated with social stress in a sex- and subtype-specific manner in both mice and humans enriched for genes involved in the PI3K-Akt-mTOR signaling pathway.

Conclusion: Chronic social stress-induced sex-specific molecular signatures were uncovered in female subjects. Consensus modules across stress and clinical populations implicate alterations in MSN subtypes could contribute to MDD signatures among female populations.

Introduction

Major depressive disorder, (MDD), is expected to become the foremost cause of disease burden worldwide by 2030 (Bains and Abdijadid, 2025). Treatment for MDD has limited success with 30% of patients resistant and experiencing relapses (Severe, Greden and Reddy, 2020). To uncover the mechanisms underlying vulnerability to MDD, researchers use chronic stress paradigms to model disrupted affective behaviors. Chronic social stress paradigms have face validity and better mirror the psychosocial nature of human stress (Berton et al 2006, Krishnan et al 2007, Krishnan & Nestler 2010, Sial et al 2015, Francis and Lobo 2017, Iniguez et al 2018, Patel, Kas, Chattarji, Buwalda 2019).

A significant limitation of these paradigms is their use in only male animals (Seney, Glausier, Sibille 2022). Given sex differences in MDD symptomatology, antidepressant response, and increased incidence in women, female subjects are crucial for understanding MDD neuropathology (Seney, Glausier, Sibille 2022). The chronic witness defeat stress (CWDS) paradigm adapts the chronic social defeat stress paradigm (CSDS) by exposing mice to witnessed, rather than experienced, physical defeat, allowing researchers to model affective dysfunction in females (Iniguez et al 2018, Warren et al 2013, Franco et al 2022).

Understanding neurobiological mechanisms in brain regions mediating depression symptoms is essential for novel therapies. One such region is the nucleus accumbens (NAc), a key integration center in the motivational circuitry (Nestler 2015, Francis & Lobo 2016, Fox & Lobo 2019). MDD patients show reduced NAc volume and blunted activation while deep brain stimulation of the NAc reduces depression and anxiety in treatment-resistant depression (Ding et al 2022). This has led to interest in targeting the NAc for MDD treatment. Medium spiny neurons (MSNs) make up over 90% of NAc neurons and include D1- and D2-type subtypes distinguished by dopamine receptor expression and other GPCRs like adenosine 2a receptor (A2A) (Gerfen & Keefe 1994, Smith, Lobo, Spencer & Kalivas 2013). Activation of D1-MSNs promotes reward behavior, while inhibition increases vulnerability to anhedonia (Francis et al 2015, Coccurello, 2019). Increased D1-MSN intrinsic excitability and reduced synaptic input, while enhanced D2/A2A-MSN synaptic input, is associated with social avoidance and stress susceptibility (Francis et al 2015). However, how sex differences in these subtypes contribute to MDD remains unclear.

Using female CWDS and celltype-specific RNA-seq via D1-Cre-RiboTag and A2A-Cre-RiboTag mice, we profiled NAc MSN subtype-specific translatomes. We identified differentially expressed genes and co-expression networks in D1- and A2A-MSNs of stress-susceptible and resilient females. We then used publicly available transcriptomics data to identify consensus networks in male and female mice and human MDD patients, identifying unique sex-specific molecular signatures relevant to MDD (Kim et al 2024, Labonte et al

2017). Given the chronic and high relapse rates of MDD, this study may uncover foundational molecular targets for MDD and other stress-related psychiatric disorders.

Materials and Methods

Animals

Experiments followed Institutional Animal Care and Use Committee guidelines at University of Maryland School of Medicine (UMSOM). Mice were given ad libitum food/water and housed in a 12:12 h light: dark cycle in the UMSOM vivarium. Homozygous Rpl22HA ("RiboTag", RT) mice crossed with D1-Cre (line FK150)/A2A-Cre (line KG 139) mice generated female D1-Cre-RT & A2A-Cre-RT mice that were used for subtype-specific RNA-seq (Sans et al 2019). All transgenic mice were on a C57Bl/6 background and 8-10 weeks old at the start. Male CD-1 retired breeders (>4 months, Charles River) served as CWDS aggressors; male C57BL6 conspecifics were intruders.

Chronic Witness Defeat Stress (CWDS)

CWDS was performed as described (Franco et al 2022). Female experimental mice, housed behind a plexiglass divider in a cage, witnessed a male CD-1 defeat a male intruder for 10 min. The witness mouse was then housed opposite a novel CD-1 for 24-hour sensory interaction. This process was repeated for 10 days with a novel CD-1 resident each day. Control mice were pair-housed with sex-matched conspecifics, separated by a divider, for 10 days.

Three-chamber Social Interaction Test

24 hours post-defeat, mice underwent 3 chamber social interaction (3ChSI) testing. Mice started in the center of a three-chambered arena (60 × 40 cm), with empty cups in the peripheral chambers and explored the arena for 5 minutes. A sex-matched conspecific was then placed under one cup, and the same mouse explored for 5 more minutes. Time spent in the social chamber was video-tracked (TopScan Lite, CleverSys) to assess stress phenotype. Classification was based on control mice's average social chamber time (~144s). Mice spending <144s were classified as low social interactors or "susceptible," while ≥144s were classified as high social interactors or "resilient." ANOVA followed by Tukey's post hoc test assessed stress group effects in each MSN subtype.

Tissue collection & RNA isolation

24h after social interaction testing, four 14 gauge punches containing NAc were collected from D1-Cre-RT and A2A-Cre-RT mice and snap frozen at -80C. Polyribosomes were immunoprecipitated as previously described (Fox et al 2023), each sample consisting of pooled tissue from four mice with similar SI ratios. Homogenates were incubated with 5 µl anti-HA antibody (Biolegend 901515) at 4°C overnight with rotation. Samples were then incubated with 400 uL of protein G magnetic beads (Life Technologies, Carlsbad, CA, USA #100.09D) overnight at 4°C with constant rotation. Beads were washed in a magnetic rack with high-salt buffer. RNA was extracted with a DNase step (Qiagen, Germantown, MD, USA) using the RNeasy mini kit (qiagen) by adding RLT and following manufacturer instructions. RNA concentration and quality were assessed via Bioanalyzer (Agilent).

Library preparation and analysis

Samples with RNA integrity number >8 were used and pooled into biological quintuplicates for sequencing at the Maryland Genomics core of the UMSOM Institute for Genome Sciences (IGS) and processed as described previously (Engeln et al 2021). Libraries were prepared from 10 ng of RNA from each sample using the SMART-Seq v4 kit (Takara). Samples were sequenced on a NovaSeq6000 with 100 bp paired-end reads. Reads were aligned to the mouse genome (Mus musculus. GRCm38) using HISAT2 and the number of reads that aligned to the predicted coding region was determined using HTSeq (GEO submission in process).

We used two approaches to characterize transcriptomic alterations. First, we used edgeR's likelihood ratio test to identify DEGs by stress group in MSN subtypes. Genes with False Discovery Rate (FDR) < 0.05 were considered differentially expressed. Gene Ontology (GO) enrichment was performed using R packages 'gprofiler2' and 'clusterProfiler' and the online tool 'DAVID'. We next used weighted gene co-expression network analysis (WGCNA) to identify networks of co-expressed genes in D1- and D2-MSNs. 'blockwiseModules()' identified signed modules using biweight midcorrelation, power = 12, and minimum module size = 25. Module membership scores were calculated by correlating gene expression with module eigengene. Hub genes were defined as those with highest membership scores in each module. Using the R package 'limma', differentially regulated modules were identified using module eigengenes as the output variables in a linear model using design matrices to compare the stress groups. Significant modules were characterized using the same enrichment tools.

RNA-seq data from male D1- and D2-Cre-RiboTag mice and from human male and female NAc postmortem tissue were obtained from GEO (GSE147640: Kim et al 2021 and GSE102556: Labonte et al 2017, respectively). For the data from male mice, we downloaded raw sequencing reads. Preprocessing, alignment and feature counting were performed using the R package RSubread with GRCm39. For the human data, we downloaded processed read counts.

Consensus module detection and analysis

Human genes were mapped to their mouse orthologs using the R package 'orthogene'. For each dataset, genes with low counts were filtered using the edgeR command *filterByExpr*, and normalization was performed using variance stabilizing transformation. Consensus modules were constructed with all datasets using power = 8 and minimum module size = 30. The R package 'limma' was used to identify differentially regulated modules between the groups in each dataset.

Results

Social stress in females induces differentially enriched translatomes in nucleus accumbens neuron subtypes

Female D1-Cre-RT and A2A-Cre-RT mice underwent 10 days of CWDS and three chamber social interaction test on day 11 (Fig 1A). Classified as high- /low-social interactors (SI) was based on the average time controls spent in the social chamber (~144 seconds). ANOVA confirmed significant differences in interactions times between stress groups (D1: p-value < 0.05, F(2,57) = 45.09; A2A: p-value < 0.05, F(2,58) = 25.12, Fig 1B). On day 12 NAc tissue was isolated, HA-tagged polyribosomes immunoprecipitated from D1- or A2A-MSNs, and ribosome-associated RNA isolated and sequenced.

We found 9 differentially expressed genes (DEGs) in D1-MSN and 630 in A2A-MSN across stress groups (FDR < 0.05, Fig 1C, Fig S1A-B, Table S1). 7 of the D1-MSN DEGs differ between the high and low SI group with one upregulated in low SI (Fig 1C, top & far right). The top three upregulated genes – *Lars2, Abcc9* and *Kcnj8* -participate in cellular responses to energy deficiency, including an ATP-sensitive inward-rectifying potassium (KATP) channel. Other upregulated genes are involved in adhesion/migration. Enrichment analysis of upregulated low vs high SI female D1-MSN DEGs include terms such as "ATPase-coupled transmembrane transporter activity" and "potassium import across membrane" while downregulated DEGs are involved in ion transport (Fig 1D). Enrichment analysis also indicates an increase in translation in high SI female mice and DNA damage response in low SI mice (Table S2).

A2A-MSNs had more DEGs. In low-SI vs. control/high-SI females, upregulated genes were linked to junction formation, while downregulated genes were involved in synaptic transmission, particularly GPCR signaling (Fig 1C, bottom). In high SI vs control, two ribosomal subunit pseudogenes were differentially regulated. Enrichment analysis showed upregulated genes in low-SI mice were associated with structural development and transcription regulation (Fig 1E, Table S2). Downregulated genes in low SI vs control/high SI genes were enriched for synaptic processes, notably GPCR signaling (Fig 1E). There is little correlation between the MSN subtypes in gene expression change (Fig S1C).

Female social stress results in altered gene networks in nucleus accumbens neuron subtypes

Weighted Gene Co-expression Network Analysis (WGCNA) of female D1- and A2A-Cre-RT transcriptomes identified 43 D1-MSN and 21 A2A-MSN modules (Fig. 2A-B, 3A-B, S2A-B, Table S3), containing between 33–3263 and 131–3064 genes, respectively (Fig. 2C, 3C). 9 D1-MSN and 5 A2A-MSN modules were significantly associated with high- or low-social interaction (Fig. 2B-C, 3B-C, Table S3). These were characterized and placed into four categories: structural processes, protein synthesis, synapse/signaling and mitochondria related (Fig 2D, 3D, Table S4). WGCNA was also applied to chronically stressed male MSN subtypes and human NAc MDD datasets, identifying seven D1- and one D2-MSN module associated with social interaction, and 12 human NAc modules significant by sex, condition, or both (Fig S3-S5, Table S5-8).

Significant modules across female stress groups highlight the diverse effects of chronic social stress on MSN transcriptomes. While both female SI groups show differential regulation in D1-MSN modules, A2A-MSN modules are primarily affected in low SI females (Fig 2B, 3B). In contrast, male CSDS data show D1-MSN modules primarily impacted in low SI mice with one D2-MSN module upregulated in both stress groups (Fig S3B, Fig S4B).

Protein turnover modules, F D1 M20 and F A2A M3, are downregulated in low vs high SI (Fig 2D, 3D).

Protein synthesis modules

F D1 M20 hub genes regulate transcription elongation, RNA degradation, and cytoskeletal dynamics, whereas F A2A M3 hub genes involve tRNA loading, RNA splicing, and cell adhesion (Fig 2D, 3D, Table S3). Enrichment results support these findings, with F D1 M20 linked to elongation, ribosome, and proteasome function, and F A2A M3 to localization and transport terms (Table S4).

Multiple significant female modules highlight modulatory processes in protein synthesis and transport. The F D1 M28 module, downregulated in high SI vs controls, includes ribosomal subunit pseudogenes and stress response genes, (such as Rgs2, Manf, Isg15), suggesting ribosomal dysfunction (Fig 2D, Table S3-4). F D1 M36 is enriched for transcription regulation, Golgi function and RNA polymerase II activity while the F A2A M6 module is enriched for RNA polymerase II activity and ER-related terms (Fig 2D, 3D, Table S4). F D1 M36 is downregulated in high SI vs control, whereas F A2A M6 is upregulated in low vs high SI mice (Fig 2D, 3D). These findings suggest that while regulatory and dysfunctional protein production processes are reduced in D1-MSNs of high SI females, transcriptional regulation is increased in A2A-MSNs of low SI females, affecting distinct aspects of protein synthesis.

Structural modules

Structural regulation modules are exclusive to D1-MSNs. The F D1 M12 module, upregulated in low SI, includes hub genes involved in adhesion/migration, GPCR signaling, and stress response, with enrichment in adhesion/migration and cytokine activity (Fig 2D, Table S4). Another low SI-upregulated module, F D1 M35, supports junction formation and maintenance, with hub genes and enrichment linked to dendrite organization and adhesion (Fig 2D, Table S4). In contrast, F D1 M31, downregulated in high SI, regulates structural processes, featuring genes enriched for cytoskeletal/membrane functions and hub genes in lipid trafficking, cytoskeletal organization, and growth factor signaling (Fig 2D, Table S4). A similar male module, M D1 M22 is upregulated in low SI males, suggesting sex differences in structural regulatory mechanisms (Fig S3D, Table S5-6). These findings suggest increased neurite-forming activity in low SI females, while high SI females show reduced membrane and structural maintenance in D1-MSNs.

Synaptic modules

Two D1- and three A2A-MSN modules involve synaptic function. F D1 M40, downregulated low vs high SI and upregulated high SI vs controls, includes hub genes linked to synaptic vesicle sorting and release, with enrichment in protein processing and transport (Fig 2D, Table S3-4). Similarly, F A2A M15, downregulated in low SI, involves neurotransmitter/neuropeptide vesicle release, with enrichment in protein localization and secretory granules (Fig 3D, Table S4). These results suggest reduced synaptic activity in low SI females across both subtypes, while increased D1-MSN synaptic activity in high SI females is associated with resilience. The male module M D1 M10, also synaptic-related, is

upregulated low SI vs control but downregulated in low SI vs high SI (Fig S3D, Table S5-6). F A2A M10, downregulated low SI vs controls/high SI mice, includes hub genes encoding receptors and components of receptor-mediated signal transduction. Enrichment results also indicate synaptic transduction, suggesting that the module represents synaptic input (Fig 3D, Table S3-4). The male module M D2 M20 likewise involves synaptic transduction however is upregulated in both low SI and high SI compared to control (Fig S4). These results indicate that increased D1-MSN synaptic activity correlates with high sociability in both sexes, with sex differences in A2A-MSN input signaling.

Other significant synaptic modules participate in maintenance. F D1 M41, linked to synaptic structural integrity and transport, is upregulated low vs high SI/controls (Fig 2D, Table S4). F A2A M5 includes hub genes involved in vesicle trafficking, encoding receptors/channels as well as synaptic structure formation (Fig 3D, Table S3-4). This module is also upregulated low SI vs controls, suggesting that distinct aspects of synaptic maintenance are upregulated in low SI female mice by MSN subtype. In contrast, male synaptic regulation modules, M D1 M34 and M D1 M36, are downregulated low SI vs control (Fig S3D, Table S5-6). These results suggest that the regulation/modulation of synaptic activity may underlie sex differences.

Mitochondrial modules

F D1 M18 module, upregulated high SI vs control and downregulated low SI vs high SI, includes subunits of mitochondrial respiratory chain complexes and ribosomes (cytoplasmic and mitochondrial) (Fig 2D, Table S3-4). While no comparable A2A-MSN modules were significant, mitochondrial genes appear in the transcription-related module F A2A M3 (Fig 3D, Table S3). These findings suggest reduced respiratory activity in low SI female D1-MSNs, potentially due to mitochondrial dysfunction, with possible sex differences in mitochondrial roles across MSN subtypes.

Human WGCNA results

In human MDD WGCNA results, synaptic transmission and regulation are upregulated in female controls, while synaptic development is downregulated relative to males. This pattern reverses in MDD, with synaptic development downregulated in females. Mitochondrial and immune/inflammatory modules are upregulated in females in both control and MDD groups (Fig S5, Table S7-8).

Female D1- and A2A-MSN modules with the largest proportion of differentially expressed genes share common regulatory components

Modules with the highest DEG proportions were selected for analysis. F D1 M12, upregulated in low vs high SI, includes hub genes involved in adhesion and cell-matrix interaction (Fig 4A, Table S3-4). DEGs include Vtn (adhesion), KATP channel genes, and Lars2 (mitochondrial aminoacyl-tRNA synthetase), all upregulated in low vs high SI. A2A M10, downregulated in low SI females vs controls/high SI, includes downregulated DEGs involved in synaptic signaling (Fig 4B, Table S3-4). Enrichment analysis links D1 M12 and A2A M10 to PI3K-Akt-mTOR signaling (Fig 4C). Genes with high membership scores were analyzed for transcriptional regulation (Fig 4D). Nf1 and Klf6 emerged as key regulators. Enrichment

analysis revealed that Nf1-regulated D1 M12 genes are linked to cell migration and growth factor signaling, while Nf1-regulated A2A M10 genes are enriched for synaptic functions (Fig 4E).

Consensus modules

Consensus module analysis was performed using the female CWDS dataset with the male CSDS and human postmortem MDD datasets. 4029 genes overlapped across the processed datasets (Fig 5A,B, Table S9). After module construction, relationship to experimental groups was assessed. One module, module 3, is differentially regulated in both male and female socially stressed mice and in human MDD patients (Fig 5C-E). Multiple individual Module 3 hub genes are involved in transcription regulation and signal transduction – particularly the PI3K/Akt signaling pathway (Table S9). Enrichment analysis shows that the module is involved in transport and synaptic development as well as inositol phosphate activity (Fig 5E, Table S10). The genes with positive module scores, representing member genes that are expressed in the same direction as the module trend, display enrichment for synaptic activity and phosphatidylinositol-mediated signaling while the genes with negative module scores are enriched for structural and translation terms.

Discussion

We investigated sex-specific effects of chronic social stress on NAc MSN subtype transcriptomes. Using female D1-Cre-RT and A2A-Cre-RT mice exposed to CWDS, we identified unique DEGs and co-expression networks linked to social interaction phenotype, as well as networks showing sex-specific regulation in mice and humans.

Genes upregulated in D1-MSNs of low-SI females suggest altered respiratory activity. Two encode ATP-sensitive potassium channels (KATP), which regulate excitability based on ATP levels, and one, *Lars2*, encodes a mitochondrial aminoacyl-tRNA synthetase. KATP expression increases under hypoxia, while altered mt-aaRS expression is linked to mitochondrial dysfunction (Soundarapandian et al., 2007; Sissler et al., 2017). These findings align with mitochondrial changes in D1-MSNs associated with depressive-like behavior and social deficits (Gebara et al., 2021; Hollis et al., 2015). Our DEGs suggest mitochondrial dysfunction contributes to low SI in females. Additionally, a mitochondrial biogenesis module is downregulated in low-SI and upregulated in high-SI vs. controls. WGCNA also shows downregulation of co-expression networks for energy-demanding processes like protein synthesis, transport, and synaptic release in low-SI D1-MSNs.

There were far more DEGs in female A2A-MSNs relative to D1-MSNs. In low-SI females, top upregulated A2A-MSN genes are involved in structure and transcription, while top downregulated genes relate to synaptic activity, consistent with enrichment analysis results. Our previous studies show that male low social interacting mice display increased frequency of excitatory input and number of thin and stubby spines on A2A-MSNs (Francis et al, 2015; Fox et al, 2020). WGCNA identified multiple A2A-MSN gene co-expression networks impacted by chronic social stress that are involved in synaptic processes. Although synaptic input and release modules are downregulated in low-SI female mice, synapse development/formation is upregulated, possibly as a compensatory mechanism.

We identified sex differences when comparing the female CWDS results with the male CSDS modules. In D1-MSNs, differences were observed between structural regulation modules. While F D1 M31 is downregulated in high SI females, M D1 M22 is upregulated in low SI males. Both modules involve cytoskeletal regulation and lipid processing; however, F D1 M31 emphasizes growth factor signaling, whereas M D1 M22 involves more lipid processing. In A2A-MSNs, the differences were in synaptic input. F A2A M10 is downregulated in low SI vs control /high SI females while M D2 M20 is upregulated in low SI males. Although only a few genes overlap, hub genes in both modules regulate GPCR signaling, vesicle transport, and cytoskeletal dynamics. Sex differences in MSN morphology and connectivity have been reported; however, the explanation remain unclear (Forlano and Wooley, 2010). It is likely that these modules represent the mechanisms underlying the sex differences in dendritic morphology and synaptic connectivity previously reported in the NAc.

In D1-MSNs, the D1 M12 module contains the highest proportion of DEGs, with upregulation in low vs high SI groups. Multiple hub genes from this module encode proteins involved in migration. Vitronectin, a glycoprotein regulating cell adhesion and migration, is upregulated in low SI females (Ruzha et al, 2022). Other hub genes are involved in G-protein coupled receptor (GPCR) signaling and cellular homeostasis. Stress-induced depressive behaviors are linked to D1-MSN dendritic atrophy via GTPase RhoA upregulation(Fox et al., 2018). Given its involvement in GPCR signaling and cytoskeletal regulation, D1 M12 likely contributes to this atrophy in low-SI mice.

Among differentially regulated A2A-MSN modules, A2A M10 had the highest proportion of DEGs. Its hub genes, involved in synaptic and GPCR signaling, include *Oxtr* and *Resp18*, both downregulated in low-SI mice, suggesting reduced peptidergic signaling (Atari et al., 2019). *Oxtr* encodes the oxytocin receptor, linked to social reward and expressed in both D1- and A2A-MSNs (Dolen et al., 2013). All low vs. high SI DEGs in A2A M10 were downregulated and enriched for synaptic terms. The module itself was downregulated in low-SI vs. controls and high-SI females. Prior studies show increased excitatory input onto A2A-MSNs in low-SI mice post-defeat (Francis et al., 2015), suggesting reduced A2A M10 activity may reflect weakened modulatory synaptic input.

Enrichment analysis revealed that both D1 M12 and A2A M10, oppositely regulated in low SI, are significantly enriched for the PI3K-Akt pathway, involved in cell growth and survival (Sánchez-Alegría, 2018). It may also play a neuroprotective role under cellular stress (Goyal et al., 2023). The PI3K-Akt genes in D1 M12 are associated with the MAPK/ERK pathway. Dendrite morphogenesis involves both the PI3K and the MAPK pathway and that PI3K-dependent dendritic remodeling plays a neuroprotective role (Kumar et al., 2005 & Mutti et al 2022). The D2 M10 genes linked to PI3K/Akt center on synaptic signal transduction. This, again, is consistent with previous studies which have established that the PI3K/Akt pathway is involved in various components of synaptic activity (Sanchez-Alegria et al., 2018).

Consensus module analysis of the female CWDS, male CSDS, and human MDD datasets identified module 3 as sex-specific in both mice and humans. The hub genes in this module are involved in transcription regulation and the PI3K-Akt signaling pathway while enrichment analysis indicated involvement in the mTOR signaling pathway, downstream of

PI3K-Akt. Abnormal PI3K-Akt pathway activity in the NAc is linked to multiple substance use disorder conditions (Neasta et al., 2011; Hong et al., 2016; Huang et al., 2018; Zhu et al., 2021). Some studies suggest sex-specific in the NAc (Cozzoli et al., 2016; Finn et al., 2018). Although further research is required, it is likely that PI3K/Akt signaling in the NAc plays a contributing role to MDD and its sex disparity and may be considered when therapeutically targeting male or female subjects for treatment.

iRegulon analysis identified key transcriptional regulators, notably NF1 (Neurofibromin 1), as a shared regulator of F D1 M12 and F A2A M10 modules (Fig 4D). NF1, a tumor suppressor, influences migration, cytoskeletal dynamics, and stress responses through pathways including Ras/MAPK, Raf/MEK/ERK, PI3K/AKT/mTOR, and cAMP/PKA (Fig 4E; Baez-Flores et al., 2023). It also contributes to reward and motor behavior via its role in D1- and A2A-MSNs and is linked to striatal neuropsychiatric conditions (Sutton et al., 2019; Xie et al., 2017). NF1 may act as a signaling hub for GPCR pathways and could mediate stress-induced effects on MSN subtypes via PI3K/AKT/mTOR signaling.

In conclusion, chronic stress affects MSN subtypes in a cell-type- and sex-specific manner. Morphological, synaptic, mitochondrial, and transcriptional changes contribute to female vulnerability, potentially driven by PI3K/Akt/mTOR signaling and NF1. By identifying sex-specific molecular signatures in NAc MSN subtypes after social stress, this study offers key insights into MDD mechanisms and highlights potential targets for sex-informed therapies.

Declaration of interests

The authors of the paper have no financial or personal potential conflicts of interest

Legends for tables and figures

Fig 1. A) Schematic of experimental design. D1-Cre-RT and A2A-Cre-RT female mice underwent the witness defeat paradigm for 10 days (10 minutes/day). 24 hours following the last defeat, the mice went through the 3 Chamber Social Interaction Test (3ChSI) after which they were sacrificed 24h later. B) (left) Heatmap displaying localization of low social interactors (SI), high SI and control mice during the 3ChSI test. Areas highlighted in purple correspond with locations mice spend more time in while areas in yellow correspond with areas mice spent less time in. (right) Boxplots showing the time mice from each group spent in the interaction chamber (for each MSN subtype; one-way ANOVA: D1: p-value < 0.05, $F(2,57) = 45.09$; A2A: p-value < 0.05, $F(2,58) = 25.12$). The red dotted line represents the control group average, which was used to classify mice as low or high SI. C) (left to right) Venn diagrams visualizing the overlapping DEGs across stress groups in (top) D1- and (bottom) A2A-Cre-RT mice, bar plots of top differentially expressed genes (DEGs) between the stress groups in (top) D1- and (bottom) A2A-Cre-RT mice. D) Enrichment results for D1-MSN DEGs with the genes and terms color coded based on the DEG list they represent. E) Enrichment results for A2A-MSN DEGs with the genes and terms color coded based on the DEG list they represent.

Fig 2. A) Dendrogram of genes from the female D1-Cre-RT data with WGCNA module assignment represented in the colored bar below. B) Circos plots of the significant D1-MSN modules with each 'slice' corresponding with one module. The plot is organized based on

the module eigengene dendrogram, shown in the center, which positions related modules close to one another. Modules that aren't significant are uncolored. C) Circular bar plots of D1-MSN modules significantly associated with high or low social interaction in female socially stressed mice. The proportion of the module that includes differentially expressed genes from the D1 high SI vs low SI comparison is highlighted in purple. D) Sankey plots of significantly differentially regulated modules in the D1-MSN of female socially stressed mice; modules are renamed based on their original WGCNA module number and functional categorization based on hub gene and enrichment analysis characterization.

Fig 3. A) Dendrogram of genes from the female A2A-Cre-RT data with WGCNA module assignment represented in the colored bar below. B) Circos plots of the significant A2A-MSN modules with each 'slice' corresponding with one module. The plot is organized based on the module eigengene dendrogram, shown in the center, which positions related modules close to one another. Modules that aren't significant are uncolored. C) Circular bar plots of A2A-MSN modules significantly associated with stress susceptibility and/or resilience in female socially stressed mice. The proportion of the module that includes differentially expressed genes from the A2A resilient vs susceptible comparison is highlighted in purple. D) Sankey plots of significantly differentially regulated modules in the A2A-MSN of female socially stressed mice; modules are renamed based on their original WGCNA module number and functional categorization based on hub gene and enrichment analysis characterization.

Fig 4. Subtype-specific modules with the largest proportion of differentially regulated genes between stress group selected for further analysis. A) (left, above) boxplot visualizing expression level of F D1 M12 by stress group (left, below) bar chart visualizing the proportion of genes in the D1 M12 module that are differentially regulated between the stress groups (right, above) top hub genes from D1 M12 with change indicated to the right (right, below) enrichment results for genes differentially expressed within the module. B) (left, above) box plot visualizing expression level of F A2A M10 by stress group (left, below) bar chart visualizing the proportion of genes in the D2 M10 module that are differentially regulated between the stress groups (right, above) top hub genes from A2A M10 with change indicated to the right (right, below) enrichment results for differentially expressed module genes. C) Gene-concept network plot visualizing D1 M12 and D2 M10 genes involved in the PI3K-Akt signaling pathway. D) (top) top transcription regulators identified using top genes from D1 M12 and (bottom) A2A M10. E) Enriched terms associated with NF1-regulated modular genes.

Fig 5. A) cross-species consensus module analysis was performed using transcriptomic data from male and female MDD NAc, D1- and D2-Cre-RT male mice that had undergone the chronic social defeat stress paradigm (CSDS) and the female CWDS dataset. B) Dendrogram of consensus module analysis with module assignment represented by the colored bars below. C) Top hub genes from consensus module three Network plot visualizing the consesus module 3. D) Boxplot of module 3 expression in (top) NAc of male and female human, (middle) D1-MSN of stressed male and female mice and (bottom) A2A-MSN of stressed male and female mice E) Enrichment analysis results of positive and negative consensus module 3-scored genes

Author contribution

Conceptualization, MEF, MKL, GK; Methodology, MEF, MKL, SA, GK; Formal analysis, GK, MB; Investigation, MEF, DF, JO; Resources, MKL; Writing – Original Draft, GK, RC, MKL; Reviewing & Editing, MKL, RC, MEF, SAA; Visualization, GK; Funding Acquisition, MEF, MKL

Acknowledgements and disclosures

This study was funded by NIH R01MH106500 to MKL. We would like to thank Maryland Genomics within the UMSOM Institute for Genome Sciences for their RNA-sequencing service.

Bibliography

Atari, Ealla, Mitchel C Perry, Pedro A Jose, and Sivarajan Kumarasamy. "Regulated Endocrine-Specific Protein-18, an Emerging Endocrine Protein in Physiology: A Literature Review." *Endocrinology* 160, no. 9 (September 1, 2019): 2093–2100. https://doi.org/10.1210/en.2019-00397.

Báez-Flores, Juan, Mario Rodríguez-Martín, and Jesus Lacal. "The Therapeutic Potential of Neurofibromin Signaling Pathways and Binding Partners." *Communications Biology* 6 (April 20, 2023): 436. https://doi.org/10.1038/s42003-023-04815-0.

Bains, Navneet, and Sara Abdijadid. "Major Depressive Disorder." In *StatPearls*. Treasure Island (FL): StatPearls Publishing, 2025. http://www.ncbi.nlm.nih.gov/books/NBK559078/.

Berton, Olivier, Colleen A. McClung, Ralph J. Dileone, Vaishnav Krishnan, William Renthal, Scott J. Russo, Danielle Graham, et al. "Essential Role of BDNF in the Mesolimbic Dopamine Pathway in Social Defeat Stress." *Science (New York, N.Y.)* 311, no. 5762 (February 10, 2006): 864–68. https://doi.org/10.1126/science.1120972.

Coccurello, Roberto. "Anhedonia in Depression Symptomatology: Appetite Dysregulation and Defective Brain Reward Processing." *Behavioural Brain Research* 372 (October 17, 2019): 112041. https://doi.org/10.1016/j.bbr.2019.112041.

Cozzoli, Debra K., Moriah N. Kaufman, Michelle A. Nipper, Joel G. Hashimoto, Kristine M. Wiren, and Deborah A. Finn. "Functional Regulation of PI3K-Associated Signaling in the Accumbens by Binge Alcohol Drinking in Male but Not Female Mice." *Neuropharmacology* 105 (June 1, 2016): 164–74. https://doi.org/10.1016/j.neuropharm.2016.01.010.

Ding, Yu-Dan, Xiao Chen, Zuo-Bing Chen, Le Li, Xue-Ying Li, Francisco Xavier Castellanos, Tong-Jian Bai, et al. "Reduced Nucleus Accumbens Functional Connectivity in Reward Network and Default Mode Network in Patients with Recurrent Major Depressive Disorder." *Translational Psychiatry* 12 (June 6, 2022): 236. https://doi.org/10.1038/s41398-022-01995-x.

Dölen, Gül, Ayeh Darvishzadeh, Kee Wui Huang, and Robert C. Malenka. "Social Reward Requires Coordinated Activity of Accumbens Oxytocin and 5HT." *Nature* 501, no. 7466 (September 12, 2013): 179–84. https://doi.org/10.1038/nature12518.

Engeln, Michel, Yang Song, Ramesh Chandra, Ashley La, Megan E. Fox, Brianna Evans, Makeda D. Turner, et al. "Individual Differences in Stereotypy and Neuron Subtype Translatome with TrkB Deletion." *Molecular Psychiatry* 26, no. 6 (June 2021): 1846–59. https://doi.org/10.1038/s41380-020-0746-0.

Finn, Deborah A., Joel G. Hashimoto, Debra K. Cozzoli, Melinda L. Helms, Michelle A. Nipper, Moriah N. Kaufman, Kristine M. Wiren, and Marina Guizzetti. "Binge Ethanol Drinking Produces Sexually Divergent and Distinct Changes in Nucleus Accumbens Signaling Cascades and Pathways in Adult C57BL/6J Mice." *Frontiers in Genetics* 9 (September 10, 2018). https://doi.org/10.3389/fgene.2018.00325.

Forlano, Paul M., and Catherine S. Woolley. "Quantitative Analysis of Pre- and Postsynaptic Sex Differences in the Nucleus Accumbens." *The Journal of Comparative Neurology* 518, no. 8 (April 15, 2010): 1330–48. https://doi.org/10.1002/cne.22279.

Fox, Megan E., Ramesh Chandra, Miriam S. Menken, Emily J Larkin, Hyungwoo Nam, Michel Engeln, T. Chase Francis, and Mary Kay Lobo. "Dendritic Remodeling of D1 Neurons by RhoA/Rho-Kinase Mediates Depression-like Behavior." *Molecular Psychiatry* 25, no. 5 (May 2020): 1022–34. https://doi.org/10.1038/s41380-018-0211-5.

Fox, Megan E., and Mary Kay Lobo. "The Molecular and Cellular Mechanisms of Depression: A Focus on Reward Circuitry." *Molecular Psychiatry* 24, no. 12 (December 2019): 1798–1815. https://doi.org/10.1038/s41380-019-0415-3.

Fox, Megan E., Andreas B. Wulff, Daniela Franco, Eric Y. Choi, Cali A. Calarco, Michel Engeln, Makeda D. Turner, et al. "Adaptations in Nucleus Accumbens Neuron Subtypes Mediate Negative Affective Behaviors in Fentanyl Abstinence." *Biological Psychiatry*, Addiction Phenotypes and Mechanisms, 93, no. 6 (March 15, 2023): 489–501. https://doi.org/10.1016/j.biopsych.2022.08.023.

Francis, T. Chase, Ramesh Chandra, Danielle M. Friend, Eric Finkel, Genesis Dayrit, Jorge Miranda, Julie M. Brooks, et al. "Nucleus Accumbens Medium Spiny Neuron Subtypes Mediate Depression-Related Outcomes to Social Defeat Stress." *Biological Psychiatry* 77, no. 3 (February 1, 2015): 212–22. https://doi.org/10.1016/j.biopsych.2014.07.021.

Francis, T. Chase, and Mary Kay Lobo. "Emerging Role for Nucleus Accumbens Medium Spiny Neuron Subtypes in Depression." *Biological Psychiatry* 81, no. 8 (April 15, 2017): 645–53. https://doi.org/10.1016/j.biopsych.2016.09.007.

Franco, Daniela, Andreas B. Wulff, Mary Kay Lobo, and Megan E. Fox. "Chronic Physical and Vicarious Psychosocial Stress Alter Fentanyl Consumption and Nucleus Accumbens Rho GTPases in Male and Female C57BL/6 Mice." *Frontiers in Behavioral Neuroscience* 16 (February 10, 2022): 821080. https://doi.org/10.3389/fnbeh.2022.821080.

Gebara, Elias, Olivia Zanoletti, Sriparna Ghosal, Jocelyn Grosse, Bernard L. Schneider, Graham Knott, Simone Astori, and Carmen Sandi. "Mitofusin-2 in the Nucleus Accumbens Regulates Anxiety and Depression-like Behaviors Through Mitochondrial and Neuronal Actions." *Biological Psychiatry* 89, no. 11 (June 1, 2021): 1033–44. https://doi.org/10.1016/j.biopsych.2020.12.003.

Gerfen, Charles R., Keefe, Kristen A. Neostriatal dopamine receptors. Trends Neurosci. 1994 Jan;17(1):2-3: 7511845. doi: https://doi.org/10.1016/0166-2236(94)90022-1.

Goyal, Ahsas, Anant Agrawal, Aanchal Verma, and Nandini Dubey. "The PI3K-AKT Pathway: A Plausible Therapeutic Target in Parkinson's Disease." *Experimental and Molecular Pathology* 129 (February 1, 2023): 104846. https://doi.org/10.1016/j.yexmp.2022.104846.

Hollis, Fiona, Michael A. van der Kooij, Olivia Zanoletti, Laura Lozano, Carles Cantó, and Carmen Sandi. "Mitochondrial Function in the Brain Links Anxiety with Social Subordination." *Proceedings of the National Academy of Sciences* 112, no. 50 (December 15, 2015): 15486–91. https://doi.org/10.1073/pnas.1512653112.

Hong, Sa-Ik, Min-Jung Kim, In-Jee You, Seung-Hwan Kwon, Shi-Xun Ma, Ji-Young Hwang, Jee-Yeon Seo, et al. "Phentermine Induces Conditioned Rewarding Effects via Activation of the PI3K/Akt Signaling Pathway in the Nucleus Accumbens." *Psychopharmacology* 233, no. 8 (April 1, 2016): 1405–13. https://doi.org/10.1007/s00213-016-4231-z.

Iñiguez, Sergio D., Francisco J. Flores-Ramirez, Lace M. Riggs, Jason B. Alipio, Israel Garcia-Carachure, Mirella A. Hernandez, David O. Sanchez, et al. "Vicarious Social Defeat Stress Induces Depression-Related Outcomes in Female Mice." *Biological Psychiatry* 83, no. 1 (January 1, 2018): 9–17. https://doi.org/10.1016/j.biopsych.2017.07.014.

Kim, Hee-Dae, Jing Wei, Tanessa Call, Xiaokuang Ma, Nicole Teru Quintus, Alexander J. Summers, Samantha Carotenuto, et al. "SIRT1 Coordinates Transcriptional Regulation of Neural Activity and Modulates Depression-Like Behaviors in the Nucleus Accumbens." *Biological Psychiatry*, Depression Dimensions and Subtypes, 96, no. 6 (September 15, 2024): 495–505. https://doi.org/10.1016/j.biopsych.2024.03.017.

Kim, Hee-Dae, Jing Wei, Tanessa Call, Nicole Teru Quintus, Alexander J. Summers, Samantha Carotenuto, Ross Johnson, et al. "Shisa6 Mediates Cell-Type Specific Regulation of Depression in the Nucleus Accumbens." *Molecular Psychiatry* 26, no. 12 (December 2021): 7316–27. https://doi.org/10.1038/s41380-021-01217-8.

Krishnan, Vaishnav, Ming-Hu Han, Danielle L. Graham, Olivier Berton, William Renthal, Scott J. Russo, Quincey Laplant, et al. "Molecular Adaptations Underlying Susceptibility and Resistance to Social Defeat in Brain Reward Regions." *Cell* 131, no. 2 (October 19, 2007): 391–404. https://doi.org/10.1016/j.cell.2007.09.018.

Krishnan, Vaishnav, and Eric J. Nestler. "Linking Molecules to Mood: New Insight into the Biology of Depression." *The American Journal of Psychiatry* 167, no. 11 (November 2010): 1305–20. https://doi.org/10.1176/appi.ajp.2009.10030434.

Kumar, Vikas, Ming-Xiang Zhang, Michael W. Swank, Jeannette Kunz, and Gang-Yi Wu. "Regulation of Dendritic Morphogenesis by Ras–PI3K–Akt–mTOR and Ras–MAPK Signaling Pathways." *The Journal of Neuroscience* 25, no. 49 (December 7, 2005): 11288–99. https://doi.org/10.1523/JNEUROSCI.2284-05.2005.

Labonté, Benoit, Olivia Engmann, Immanuel Purushothaman, Caroline Menard, Junshi Wang, Chunfeng Tan, Joseph R Scarpa, et al. "Sex-Specific Transcriptional Signatures in Human Depression." *Nature Medicine* 23, no. 9 (September 2017): 1102–11. https://doi.org/10.1038/nm.4386.

Mutti, Veronica, Federica Bono, Zaira Tomasoni, Leonardo Bontempi, Adele Guglielmi, Silvia Bolognin, Jens C. Schwamborn, Cristina Missale, and Chiara Fiorentini. "Structural Plasticity of Dopaminergic Neurons Requires the Activation of the D3R-nAChR Heteromer and the PI3K-ERK1/2/Akt-Induced Expression of c-Fos and p70S6K Signaling Pathway." *Molecular Neurobiology* 59, no. 4 (2022): 2129–49. https://doi.org/10.1007/s12035-022-02748-z.

Neasta, Jérémie, Sami Ben Hamida, Quinn V. Yowell, Sebastien Carnicella, and Dorit Ron. "AKT Signaling Pathway in the Nucleus Accumbens Mediates Excessive Alcohol Drinking Behaviors." *Biological Psychiatry* 70, no. 6 (September 15, 2011): 575–82. https://doi.org/10.1016/j.biopsych.2011.03.019.

Nestler, Eric J. "Role of the Brain's Reward Circuitry in Depression: Transcriptional Mechanisms." *International Review of Neurobiology* 124 (2015): 151–70. https://doi.org/10.1016/bs.irn.2015.07.003.

Patel, Deepika, Martien J. Kas, Sumantra Chattarji, and Bauke Buwalda. "Rodent Models of Social Stress and Neuronal Plasticity: Relevance to Depressive-like Disorders." *Behavioural Brain Research* 369 (September 2, 2019): 111900. https://doi.org/10.1016/j.bbr.2019.111900.

Ruzha, Yelizhati, Junjun Ni, Zhenzhen Quan, Hui Li, and Hong Qing. "Role of Vitronectin and Its Receptors in Neuronal Function and Neurodegenerative Diseases." *International Journal of Molecular Sciences* 23, no. 20 (October 16, 2022): 12387. https://doi.org/10.3390/ijms232012387.

Sánchez-Alegría, Karina, Manuel Flores-León, Evangelina Avila-Muñoz, Nelly Rodríguez-Corona, and Clorinda Arias. "PI3K Signaling in Neurons: A Central Node for the Control of Multiple Functions." *International Journal of Molecular Sciences* 19, no. 12 (December 2018): 3725. https://doi.org/10.3390/ijms19123725.

Sanz, Elisenda, Linghai Yang, Thomas Su, David R. Morris, G. Stanley McKnight, and Paul S. Amieux. "Cell-Type-Specific Isolation of Ribosome-Associated mRNA from Complex Tissues." *Proceedings of the National Academy of Sciences* 106, no. 33 (August 18, 2009): 13939–44. https://doi.org/10.1073/pnas.0907143106.

Seney, Marianne L., Jill Glausier, and Etienne Sibille. "Large-Scale Transcriptomics Studies Provide Insight Into Sex Differences in Depression." *Biological Psychiatry*, Insight Into Sex Differences in Psychiatric Syndromes From Transcriptomic Analyses, 91, no. 1 (January 1, 2022): 14–24. https://doi.org/10.1016/j.biopsych.2020.12.025.

Severe, Jennifer, John F. Greden, and Priyanka Reddy. "Consequences of Recurrence of Major Depressive Disorder: Is Stopping Effective Antidepressant Medications Ever Safe?" *Focus* 18, no. 2 (April 2020): 120–28. https://doi.org/10.1176/appi.focus.20200008.

Sial, Omar K., Brandon L. Warren, Lyonna F. Alcantara, Eric M. Parise, and Carlos A. Bolaños-Guzmán. "Vicarious Social Defeat Stress: Bridging the Gap between Physical and Emotional Stress." *Journal of Neuroscience Methods* 258 (January 30, 2016): 94–103. https://doi.org/10.1016/j.jneumeth.2015.10.012.

Sissler, Marie, Ligia Elena González-Serrano, and Eric Westhof. "Recent Advances in Mitochondrial Aminoacyl-tRNA Synthetases and Disease." *Trends in Molecular Medicine* 23, no. 8 (August 1, 2017): 693–708. https://doi.org/10.1016/j.molmed.2017.06.002.

Smith RJ, Lobo MK, Spencer S, Kalivas PW. Cocaine-induced adaptations in D1 and D2 accumbens projection neurons (a dichotomy not necessarily synonymous with direct and indirect pathways). *Current Opinion in Neurobiology* (2013 Aug;23(4)):546-52. https://doi.org/10.1016/j.conb.2013.01.026.

Soundarapandian, Mangala M., Xiaofen Zhong, Lisheng Peng, Di Wu, and Youming Lu. "Role of KATP Channels in Protection against Neuronal Excitatory Insults." *Journal of Neurochemistry* 103, no. 5 (2007): 1721–29. https://doi.org/10.1111/j.1471-4159.2007.04963.x.

Walter, Heather J., A. Reese Abright, Oscar G. Bukstein, John Diamond, Helene Keable, Jane Ripperger-Suhler, and Carol Rockhill. "Clinical Practice Guideline for the Assessment and Treatment of Children and Adolescents With Major and Persistent Depressive Disorders." *Journal of the American Academy of Child & Adolescent Psychiatry* 62, no. 5 (May 1, 2023): 479–502. https://doi.org/10.1016/j.jaac.2022.10.001.

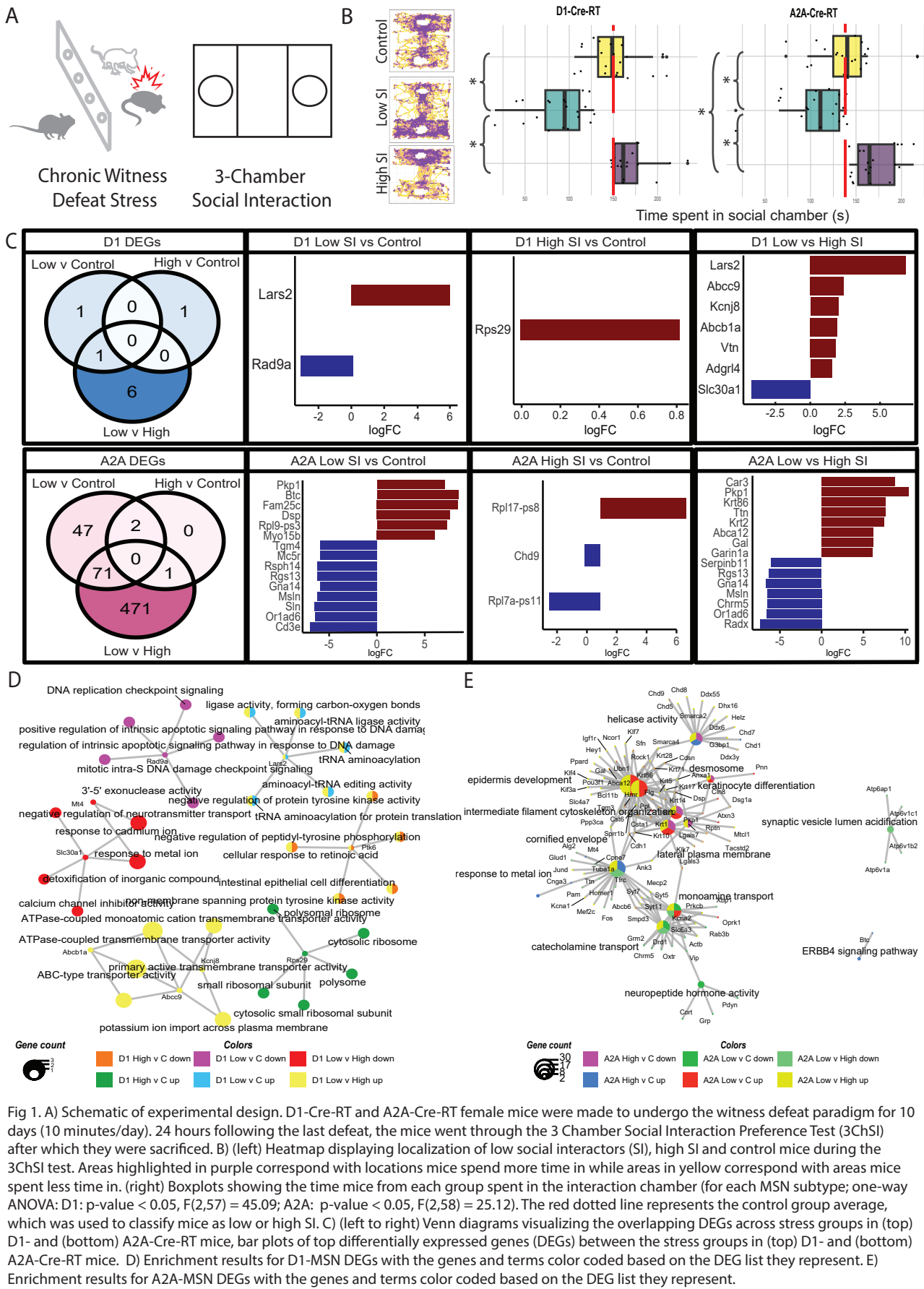

Fig 1. A) Schematic of experimental design. D1-Cre-RT and A2A-Cre-RT female mice were made to undergo the witness defeat paradigm for 10 days (10 minutes/day). 24 hours following the last defeat, the mice went through the 3 Chamber Social Interaction Preference Test (3ChSI) after which they were sacrificed. B) (left) Heatmap displaying localization of low social interactors (SI), high SI and control mice during the 3ChSI test. Areas highlighted in purple correspond with locations mice spend more time in while areas in yellow correspond with areas mice spent less time in. (right) Boxplots showing the time mice from each group spent in the interaction chamber (for each MSN subtype; one-way ANOVA: D1: p-value < 0.05, F(2,57) = 45.09; A2A: p-value < 0.05, F(2,58) = 25.12). The red dotted line represents the control group average, which was used to classify mice as low or high SI. C) (left to right) Venn diagrams visualizing the overlapping DEGs across stress groups in (top) D1- and (bottom) A2A-Cre-RT mice, bar plots of top differentially expressed genes (DEGs) between the stress groups in (top) D1- and (bottom) A2A-Cre-RT mice. D) Enrichment results for D1-MSN DEGs with the genes and terms color coded based on the DEG list they represent. E) Enrichment results for A2A-MSN DEGs with the genes and terms color coded based on the DEG list they represent.

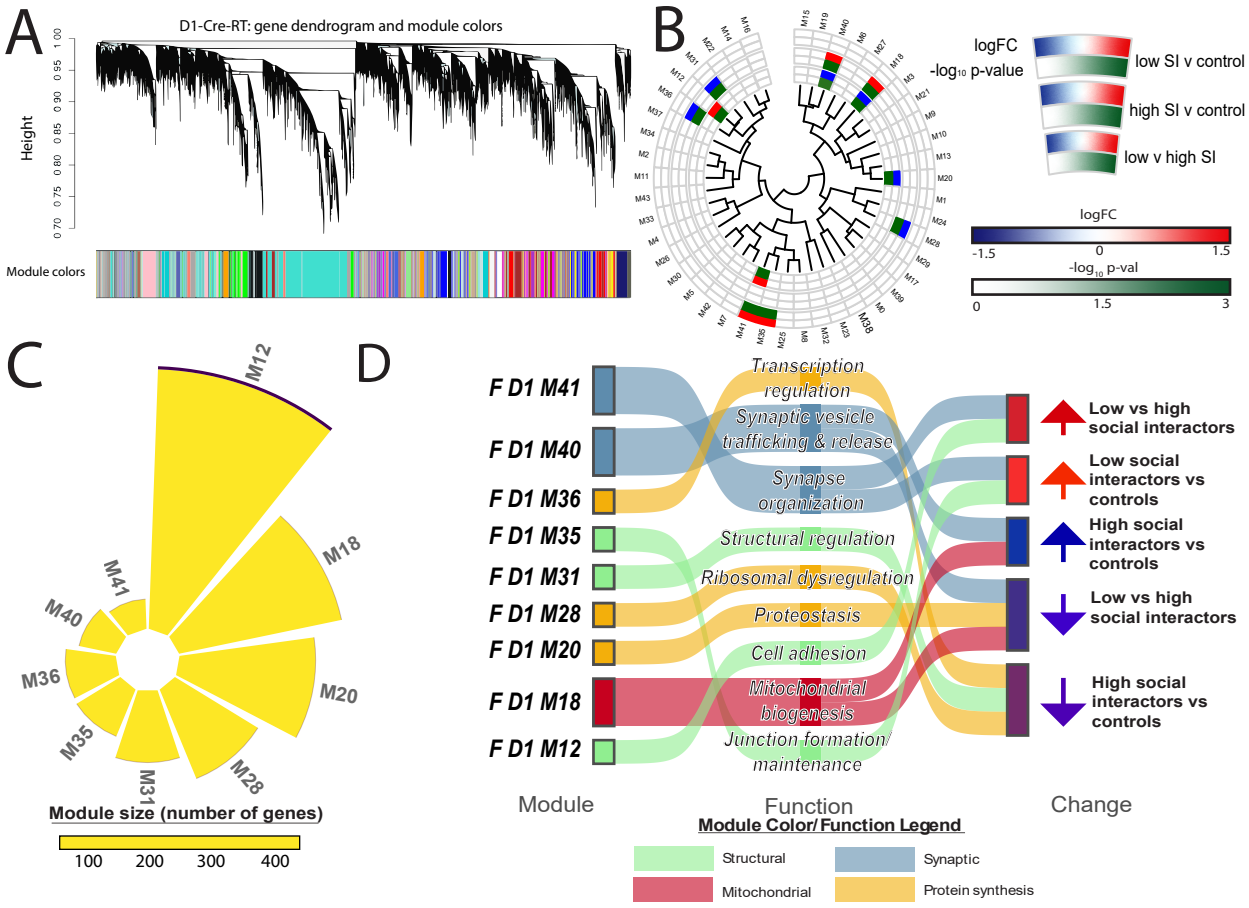

Fig 2. A) Dendrogram of genes from the female D1-Cre-RT data with WGCNA module assignment represented in the colored bar below. B) Circos plots of the significant D1-MSN modules with each 'slice' corresponding with one module. The plot is organized based on the module eigengene dendrogram, shown in the center, which positions related modules close to one another. Modules that aren't significant are uncolored. C) Circular bar plots of D1-MSN modules significantly associated with high or low social interaction in female socially stressed mice. The proportion of the module that includes differentially expressed genes from the D1 high SI vs low SI comparison is highlighted in purple. D) Sankey plots of significantly differentially regulated modules in the D1-MSN of female socially stressed mice; modules are renamed based on their original WGCNA module number and functional categorization based on hub gene and enrichment analysis characterization.

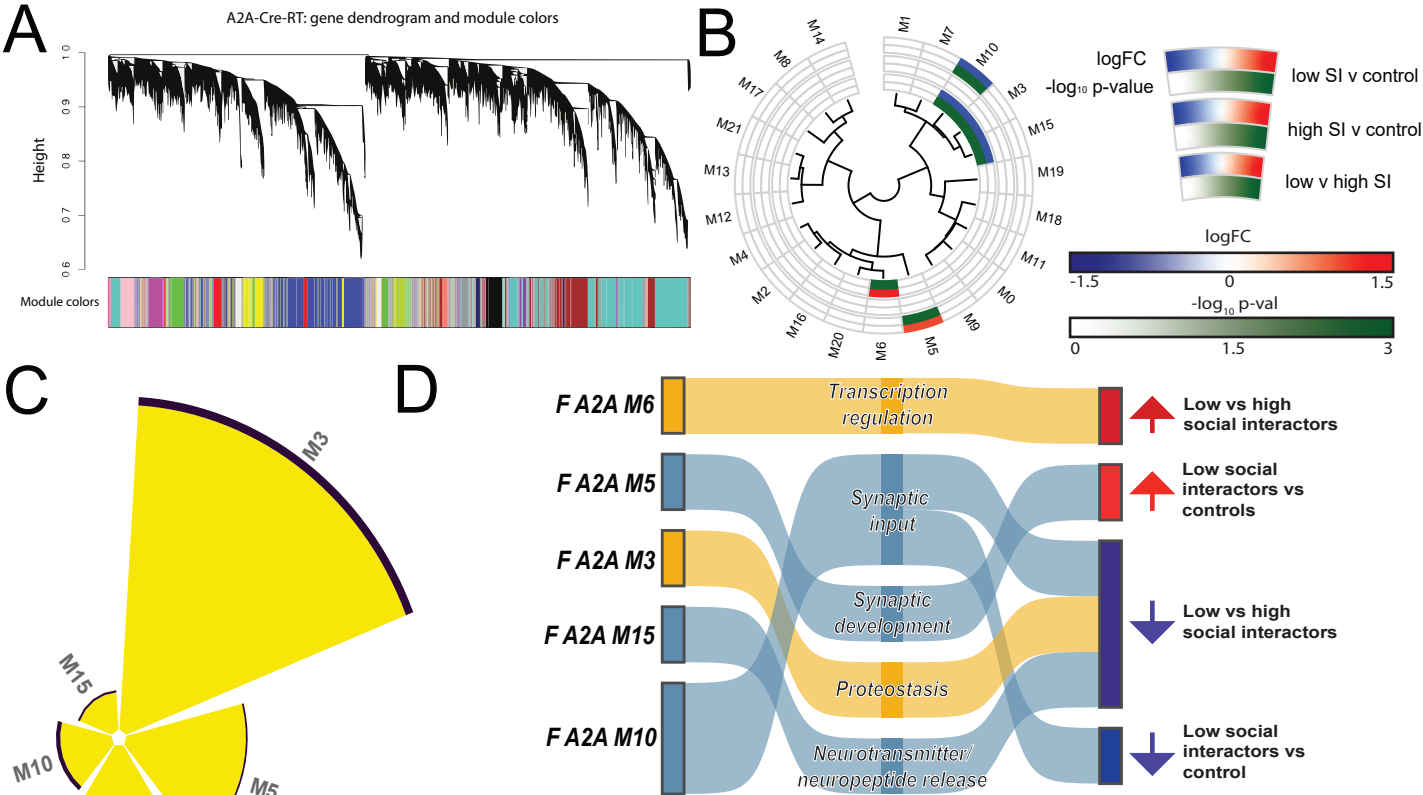

Fig 3. A) Dendrogram of genes from the female A2A-Cre-RT data with WGCNA module assignment represented in the colored bar below. B) Circos plots of the significant A2A-MSN modules with each 'slice' corresponding with one module. The plot is organized based on the module eigengene dendrogram, shown in the center, which positions related modules close to one another. Modules that aren't significant are uncolored. C) Circular bar plots of A2A-MSN modules significantly associated with stress susceptibility and/or resilience in female socially stressed mice. The proportion of the module that includes differentially expressed genes from the A2A resilient vs susceptible comparison is highlighted in purple. D) Sankey plots of significantly differentially regulated modules in the A2A-MSN of female socially stressed mice; modules are renamed based on their original WGCNA module number and functional categorization based on hub gene and enrichment analysis characterization.

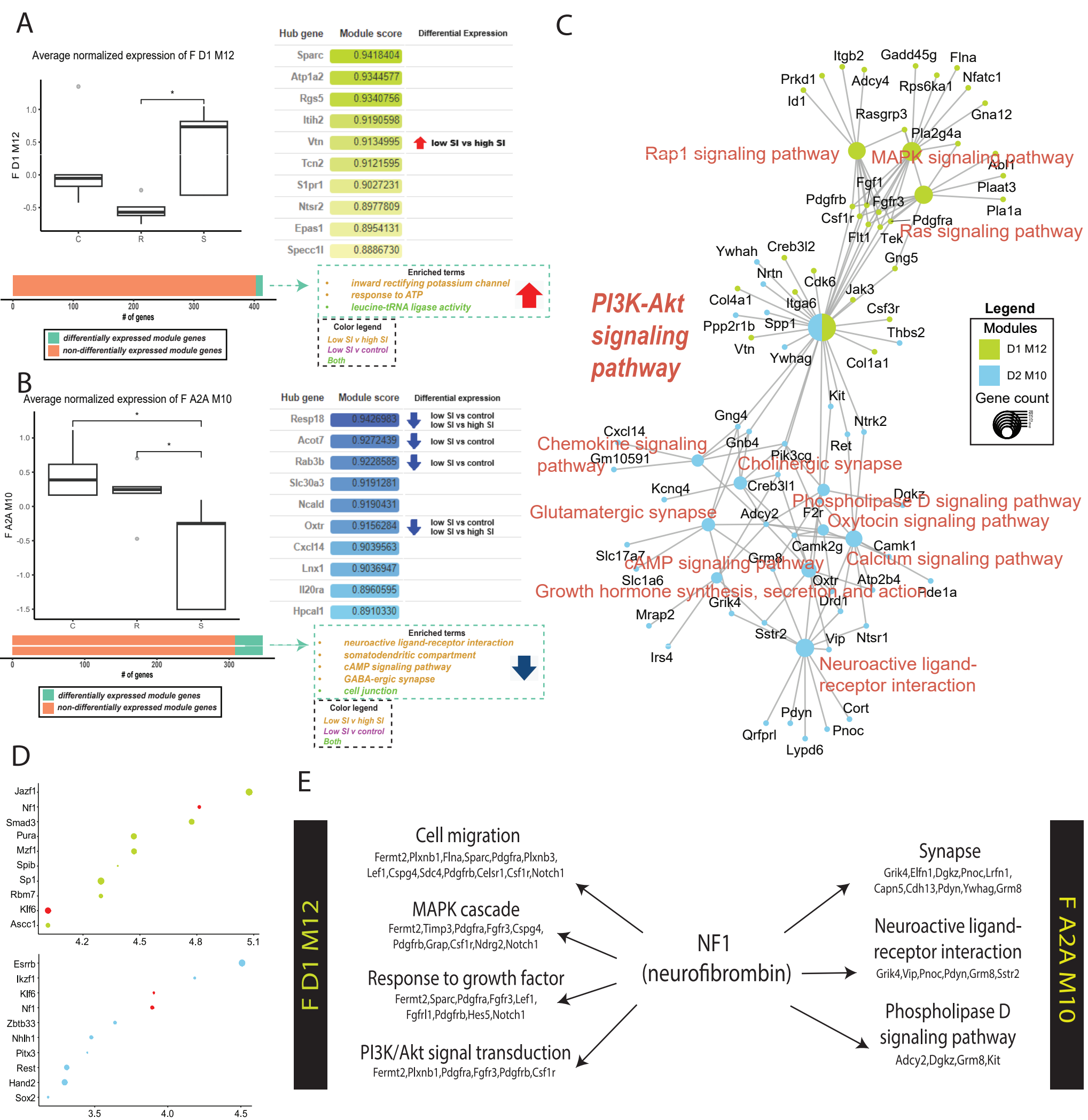

Fig 4. Subtype-specific modules with the largest proportion of differentially regulated genes between stress group selected for further analysis. A) (left, above) boxplot visualizing expression level of F D1 M12 by stress group (left, below) bar chart visualizing the proportion of genes in the D1 M12 module that are differentially regulated between the stress groups (right, above) top hub genes from D1 M12 with change indicated to the right (right, below) enrichment results for genes differentially expressed within the module. B) (left, above) network plot visualizingbox plot visualizing expression level of F A2A M10 by stress group (left, below) bar chart visualizing the proportion of genes in the D2 M10 module that are differentially regulated between the stress groups (right, above) top hub genes from A2A M10 with change indicated to the right (right, below) enrichment results for differentially expressed module genes. C) Gene-concept network plot visualizing D1 M12 and D2 M10 genes involved in the PI3K-Akt signaling pathway. D) (top) top transcription regulators identified using top genes from D1 M12 and (bottom) A2A M10. E) Enriched terms associated with NF1-regulated modular genes.

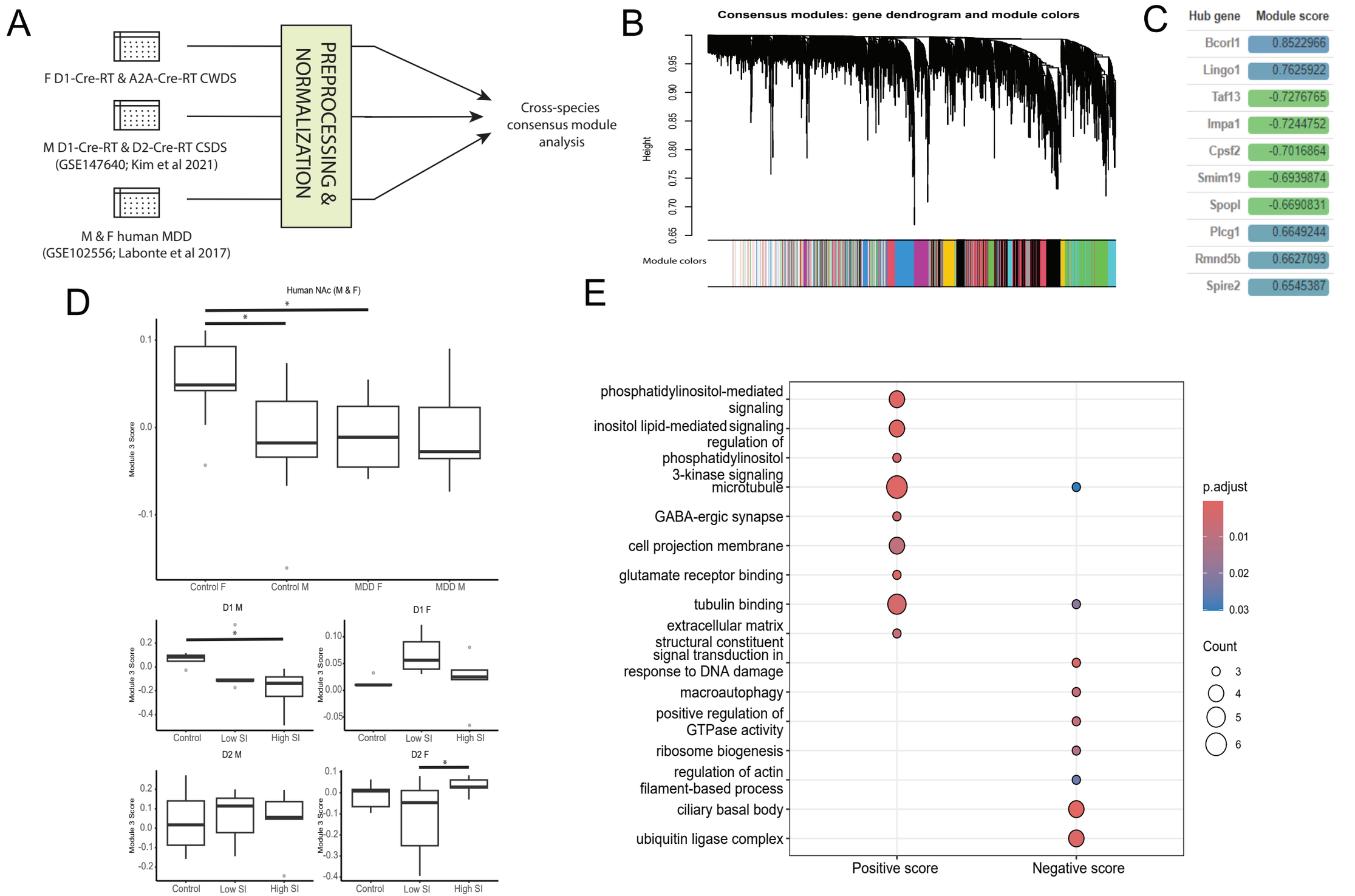

Fig 5. A) cross-species consensus module analysis was performed using transcriptomic data from male and female human NAc of MDD pateints, D1- and D2-Cre-RT male mice that had undergone the chronic social defeat stress paradigm (CSDS) and the female CWDS dataset. B) Dendrogram of consensus module analysis with module assignment represented by the colored bars below. C) Top hub genes from consensus module three Network plot visualizing the consesus module 3. D) Boxplot of module 3 expression in (top) NAc of male and female human, (middle) D1-MSN of stressed male and female mice and (bottom) D2-MSN of stressed male and female mice E) Enrichment analysis results of positive and negative consensus module 3-scored genes